J. Indones. Math. Soc.
Vol. 26, No. 01 (2020), pp. 37–54.

MODELLING EFFECTS OF HCV PLUS-STRAND RNA INFLUX INTO A CELL DURING HCV REPLICATION

Adamu Ishaku[1,2], Nafiu Hussaini*,[2]

[1]**Department of Mathematics, Faculty of Sciences, Gombe State University, Gombe, Gombe State, Nigeria.**
adammaths@gsu.edu.ng
[2]**Department of Mathematical Sciences, Faculty of Sciences, Bayero University, Kano, Kano State, Nigeria.,**
* **Corresponding author: nhussaini.mth@buk.edu.ng**

Abstract. This paper presents a subgenomic Hepatitis C Virus (HCV) replication model which incorporates the rate of influx of HCV plus-strand RNA into Huh-7 cell and monitored its effects. The model exhibits three equilibria, namely: trivial equilibrium, healthy equilibrium and endemic equilibrium. Stability analysis of the model reveals that the healthy equilibrium is globally asymptotically stable under certain condition. Furthermore, it is shown that increase in the rate of influx, increases the steady state level of total plus strand RNA, synthesized plus strand RNA, replicated plus strand RNA and NS5B in the system. Sensitivity and uncertainty analyses of the model (using the *basic replication number* ($\mathcal{R}_0$) as the response function) show that the top three PRCC-ranked parameters are the rate of influx, k_0 of HCV plus-strand RNA, the rate of production of translation complex (T_c) and the rate of degradation, μ_p^{cyt}, of plus-strand RNA R_P^{cyt}. Furthermore, the distribution of $\mathcal{R}_0$ is between [0.9999, 1.0008] with a mean of $\mathcal{R}_0 = 1.0003$.

Key words and Phrases: Hepatitis C Virus, replication, basic replication number, stability analysis.

1. INTRODUCTION

Hepatitis C Virus (HCV) is a plus-strand RNA virus that attacks liver cells and causes liver failure which can lead to liver transplantation or death [3]. HCV is often asymptomatic, only in about 15% of the cases symptoms includes lost of

2020 Mathematics Subject Classification: 4811
Received: 03-06-2018, accepted: 19-03-2019.

appetite, fatigue, nausea, muscles or joint pain, weight lost, etc. [3]. The virus is very small in size (about 30-60nm) [1], envelopes and belongs to the genus Hepacivirus in the family Flaviviridae [2]. The major route of transmitting this virus is via blood (i.e, during blood transfusion, use of poorly sterilized medical equipments that carried infected blood, etc) [3, 17]. According to WHO, about 71 million persons are infected with HCV globally and among which about 15 - 45% clear the virus within 6 months. Approximately, 399,000 individuals die every year [30].

In order understand the dynamics, prevent and control the spread of HCV within an individual (in vivo) or in a population, several mathematical models have been proposed and rigorously analysed by different authors (see, for instance, [2, 3, 8, 14, 25, 26] and references therein). Spiegelman in 1970 [4] has shown that viral RNA amplification depends on RNA polymerase-containing RNA replicase that specifically interacts with the incoming viral RNA (plus-strand). In 1981, Biebricher et al [19] used the idea developed in [4] and studied the kinetics of RNA amplification by $Q\beta$ replicase (quantitatively) and developed a kinetic model for self-replication of $Q\beta$ RNA in vitro [5].

A model for complete life cycle of $Q\beta$ has been presented in [18]. Using a subgenomic genotype 1b (Con1) replicon, Lohmann et al. in [6] found that HCV RNA replication persist in a human hepatoma cell line (Huh-7)1 . Later, the adaptive mutations in nonstructural proteins were identified by Bartenschlager et al. in [7] which improved the efficiency of HCV replication. In 2007, Dahari et al. in [2] produced a model for complete replication of HCV. In this study, the model presented by Dahari et al. in [2] is extended by incorporating the rate of influx of HCV plus-strand into a cell and monitored (mathematically) its effects to the production of more HCV particles.

This paper is organized as follows. The model is formulated in Section 2. The model analysis is presented in Section 3. Numerical simulations of the extended model are given in Section 4. Sensitivity and uncertainty analyses are performed in Section 5.

2. MODEL FORMULATION

The model is derived from the details of HCV replication life cycle as described by Dahari et al [2] and other literature in [13, 15, 17]. We sub-divide the process into three stages viz: HCV entry, HCV translation, and HCV replication.
Stage I: Hepatitis C Virus Entry
The first step of interaction between HCV and the target cell that is required for the initiation of the infection [9]. Recent studies of HCV entry revealed that the process is slow and complex multistep [11]. The virus cross the plasma membrane of the target cell and have access to cytosolic and/or nuclear components in order to replicate its genome [10]. The viral entry begins with binding of the HCV particle to an attachment factor on the cell surface [11]. After binding of the virus to the

cell surface, the virus enters the cell by clathrin-dependent endocytosis and upon acidification, fusion of the viral envelope, presumably with the membrane of an early endosome will lead to the release of the viral nucleocapsid into the cytoplasm [12].

Stage II: Translation of Hepatitis C Virus RNA

The plus-strand RNA (R_p^{cyp}) enters the cell, it interacts with the host ribosome complex (R_{ibo}) to produce translation complex (T_c) at a constant rate k_1. Once this translation complex is being produced, then translation begins and viral polyprotein (P) will be formed at a constant rate k_2. Thus, T_c degrades at a constant rate μ_{T_c}. After viral polyprotein is produced, we assume that the ribosome complex dissociate from T_c and that will result to free plus-strand RNA. This R_p^{cyp} degrades at the rate of μ_p^{cyt}. Therefore, R_p^{cyt} and R_{ibo} disappear at a rate of k_1 and then reappear at a rate k_2. The viral polyprotein alone will then split at a constant rate k_c into separate structural and non-structural viral protein. It is this non-structural viral polyprotein that include NS5B polymerase (E^{cyt}) which contains RNA replicase which is the replication machinery. Then, E^{cyt} will then degrades with rate constant μ_E^{cyt}. When NS5B is formed, then the translation is complete [2].

Stage III: Replication of Hepatitis C Virus RNA

The non-structural viral protein (NS5B polymerase) enters the VMS at a constant rate k_{Ein}. Also, the free plus-strand that dissociate from T_c will also enter the VMS at a constant rate k_{pin}. The free plus-strand in VMS (R_p) will interact with NS5B polymerase in VMS (E) to form plus-strand replicative intermediate complex (R_{Ip}) at a constant rate k_3. The produced R_{Ip} degrades at a rate μ_{Ip}. The complimentary minus-strand will then be formed at a constant rate of k_{4m} and the R_{Ip} dissociates to double strand RNA (R_{ds}) and NS5B polymerase (E). After the formation of R_{ds}, then E will act on it and leads to the formation of double strand replicative intermediate RNA (R_{Ids}) at a constant rate of k_5 and the formed R_{Ids} degrades at a constant rate of μ_{Ids}. The formed R_{Ids} produces the replicate nascent plus-strand RNA at a constant rate of k_{4p} per complex and once this nascent plus-strand RNA is replicated. The unwounded plus-strand RNA R_p is then released from R_{Ids} complex (along with R_{ds} and E). The replicated plus-strand RNA (R_P) will degrade at a constant rate of μ_p and then transported back to the cytoplasm at a constant rate of k_{pout}. Figure 1 represents the diagrammatic explanation of HCV plus-strand RNA entry, translation and replication processes. The first four equations of the model (1) describe the translation process of HCV, while the last five equations describe replication process of HCV as shown in Figure 1.

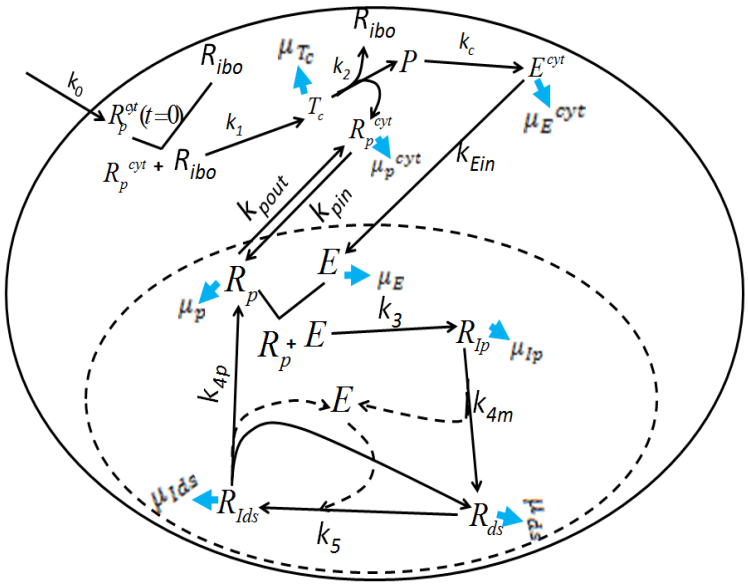

FIGURE 1. *The Reaction Scheme for HCV Replication Process in Huh-7 Cell with k_0 as Rate of Influx of HCV Plus-strand RNA. The Cell Membrane is Symbolised by a Solid Oval Shape and VMS is Symbolised by Dotted Oval Shape.*

$$
\begin{aligned}
\frac{dR_p^{cyt}}{dt} &= k_0 R_p^{cyt} + k_2 T_c + k_{pout} R_p - k_1 R_{ibo} R_p^{cyt} - k_{pin} R_p^{cyt} - \mu_p^{cyt} R_p^{cyt} \\
\frac{dT_c}{dt} &= k_1 R_{ibo} R_p^{cyt} - k_2 T_c - \mu_{T_c} T_c \\
\frac{dP}{dt} &= k_2 T_c - k_c p \\
\frac{dE^{cyt}}{dt} &= k_c P - k_{Ein} E^{cyt} - \mu_E^{cyt} E^{cyt} \\
\frac{dR_p}{dt} &= k_{4p} R_{Ids} + k_{pin} R_p^{cyt} - k_3 R_p E - k_{pout} R_p - \mu_p R_p \\
\frac{dR_{ds}}{dt} &= k_{4m} R_{Ip} + k_{4p} R_{Ids} - k_5 R_{ds} E - \mu_{ds} R_{ds} \\
\frac{dE}{dt} &= k_{Ein} E^{cyt} + k_{4m} R_{Ip} + k_{4p} R_{Ids} - k_3 R_p E - k_5 R_{ds} E - \mu_E E \\
\frac{dR_{Ip}}{dt} &= k_3 R_p E - k_{4m} R_{Ip} - \mu_{Ip} R_{Ip} \\
\frac{dR_{Ids}}{dt} &= k_5 R_{ds} E - k_{4p} R_{Ids} - \mu_{Ids} R_{Ids}
\end{aligned}
\tag{1}
$$

with the initial conditions

$$R_p^{cyt}(0) \geq 0, \quad T_c(0) \geq 0, \quad P \geq 0, \quad E^{cyt} \geq 0, \quad R_p \geq 0,$$
$$R_{ds} \geq 0, \quad E \geq 0, \quad R_{Ip} \geq 0, \quad R_{Ids} \geq 0.$$

Parameter	Description	Range/value	Citation
k_1	Rate of T_c formation	$34 - 83$	[2]
k_2	polyprotein translation rate	100	Assumed
k_3	R_{Ip} formation rate	$0.01 - 0.02$	Assumed
k_{4p}	R_P synthesis rate	1.7	Assumed
k_{4m}	R_{ds} synthesis rate	1.7	Assumed
k_5	R_{Ids} formation rate	$4\ molecule^{-1}$	[2]
k_{pout}	Rate of transporting R_P into cytoplasm	0.2	[2]
k_{pin}	Rate of transporting R_P^{cyt} into VMS	0.2	[2]
k_{Ein}	Rate of transporting E^{cyt} into VMS	4×10^{-6} - 4×10^{-5}	[2]
k_c	Viral polyprotein cleavage rate	$0.2 - 1$	[2]
μ_p^{cyt}	R_P^{cyt} degradation rate	$0.06 - 15$	Assumed
μ_p	R_P degradation rate	0.07	[22]
μ_{ds}	R_{ds} degradation rate	0.06	[23]
μ_{Ip}	R_{Ip} degradation rate	$0.01 - 0.06$	Assumed
μ_{Ids}	R_{Ids} degradation rate	0.13	[2]
μ_{T_c}	T_c degradation rate	$0.001 - 0.02$	Assumed
μ_E	E degradation rate	$0.001 - 0.06$	Assumed
μ_E^{cyt}	E^{cyt} degradation rate	0.06	[23]
$R_P^{cyp}(0)$	Initial quantity of plus-strand RNA	500	[2]
R_{ibo}^{Tot}	Number of ribosome complex	700	[2]

TABLE 1. Parameter description and values for model (2) model

3. MODEL ANALYSIS

For simplicity, let $R_p^{cyt} = x_1$, $T_c = x_2$, $P = x_3$, $E^{Cyt} = x_4$, $R_p = x_5$, $R_{ds} = x_6$, $E = x_7$, $R_{Ip} = x_8$, and $R_{Ids} = x_9$ in equation (1), we have:

$$\begin{aligned}
\frac{dx_1}{dt} &= k_0x_1 + k_2x_2 + k_{pout}x_5 - k_1R_{ibo}x_1 - k_{pin}x_1 - \mu_p^{cyt}x_1\\
\frac{dx_2}{dt} &= k_1R_{ibo}x_1 - k_2x_2 - \mu_{T_c}x_2\\
\frac{dx_3}{dt} &= k_2x_2 - k_cx_3\\
\frac{dx_4}{dt} &= k_cx_3 - k_{Ein}x_4 - \mu_E^{cyt}x_4\\
\frac{dx_5}{dt} &= k_{4p}x_9 + k_{pin}x_1 - k_3x_5x_7 - k_{pout}x_5 - \mu_px_5\\
\frac{dx_6}{dt} &= k_{4m}x_8 + k_{4p}x_9 - k_5x_6x_7 - \mu_{ds}x_6\\
\frac{dx_7}{dt} &= k_{Ein}x_4 + k_{4m}x_8 + k_{4p}x_9 - k_3x_5x_7 - k_5x_6x_7 - \mu_Ex_7\\
\frac{dx_8}{dt} &= k_3x_5x_7 - k_{4m}x_8 - \mu_{Ip}x_8\\
\frac{dx_9}{dt} &= k_5x_6x_7 - k_{4p}x_9 - \mu_{Ids}x_9
\end{aligned} \tag{2}$$

with the initial conditions

$$x_i(0) \geq 0, \quad i = 1, 2, 3, \ldots, 9.$$

3.1. **Positivity of solution.** Since the model monitors number of molecules of replication mechanism during HCV replication, then we need to show that for non-negative initial conditions, the variables $x_i(t)$, $i = 1, 2, \ldots, 9$ are positive and remain positive for all $t \geq 0$. Hence the following result.

Lemma 3.1. *If $x_i(0) > 0$, for $i = 1, 2, ..., 9$, then the solution $x_i(t)$, for $i = 1, 2, \ldots, 9$ of the model (2) are positive for all $t \geq 0$.*

Proof. Adopting the prove by contradiction method used in proving the positivity of solution of system of nonlinear equations in [27], we prove this lemma by contradiction.
Suppose there exists a time t_j such that

$$\begin{aligned}
x_j(t_j) = 0, \quad x_j'(t_j) < 0, \quad j = 1, 2, 3, ..., 9,\\
x_i(t) > 0 \quad i \neq j, \quad i = 1, 2, 3, ..., 9, \quad 0 < t < t_j.
\end{aligned} \tag{3}$$

Since the model parameters are positive, then from assumption (3) and :
first equation in model(2) (i.e j=1), we have

$$x_1'(t_1) = k_2x_2 + k_{pout}x_5 > 0, \tag{4}$$

second equation in model(2) (i.e j=2) , we have

$$x_2'(t_2) = k_1 R_{ibo} x_1 > 0, \tag{5}$$

third equation in model (2) (i.e j=3), we have

$$x_3'(t_3) = k_2 x_2 > 0, \tag{6}$$

fourth equation in model (2) (i.e j=4), we have

$$x_4'(t_4) = k_c x_3 > 0, \tag{7}$$

It is easy to show from assumption (3) and fifth, sixth, seventh, eighth, and ninth equations. Hence, the solutions of the model (2), $x_j(t) > 0, \quad j = 1, 2, 3, 4, 5, 6, 7, 8, 9$ remain positive for $t \geq 0$. □

Now setting the right-hand side of model (2) to zero (noting that $R_{ibo} = R_{ibo}^{Tot} - x_2$).
The following equilibria are identified.

(1) Trivial equilibrium i.e $E_0 = (0, 0, 0, 0, 0, 0, 0, 0, 0)$.
(2) Healthy equilibrium i.e when a cell is healthy (plus-strand RNA (which is x_1) is not in the cell and all other mechanisms (except T_c) are not produced and all other parameters are zeros), thus $x_1 = x_3 = x_4 = x_5 = x_6 = x_7 = x_8 = x_9 = 0$. The number of free ribosome complexes involved in HCV RNA translation is calculated in [2] as $R_{ibo} = R_{ibo}^{Tot} - T_c$, then we say $T_c = R_{ibo}^{Tot} - R_{ibo}$. Let $T_c = \eta$, then $x_2 = \eta$ where $\eta = R_{ibo}^{Tot} - R_{ibo}$, hence healthy equilibrium point $E_1 = (0, \eta, 0, 0, 0, 0, 0, 0, 0)$.
(3) Endemic equilibrium i.e $E^* = (x_1^* x_2^*, x_3^*, x_4^*, x_5^*, x_6^*, x_7^*, x_8^*, x_9^*)$.

3.2. **Local Stability Analysis.** In this section, we analyze the local stability of trivial and healthy equilibrium and give the condition for the existence of equilibrium of the model.

3.2.1. *Local stability of trivial equilibrium.* The Jacobian matrix evaluated at trivial equilibrium E_0, $J(E_0)$, is given by

$$J(E_0) = \begin{pmatrix} -a_1 & k_2 & 0 & 0 & k_{pout} & 0 & 0 & 0 & 0 \\ b_1 & -a_2 & 0 & 0 & 0 & 0 & 0 & 0 & 0 \\ 0 & k_2 & -k_c & 0 & 0 & 0 & 0 & 0 & 0 \\ 0 & 0 & k_c & -a_3 & 0 & 0 & 0 & 0 & 0 \\ k_{pin} & 0 & 0 & 0 & -a_4 & 0 & 0 & 0 & k_{4p} \\ 0 & 0 & 0 & 0 & 0 & -\mu_{ds} & 0 & k_{4m} & k_{4p} \\ 0 & 0 & 0 & k_{Ein} & 0 & 0 & -\mu_E & k_{4m} & k_{4p} \\ 0 & 0 & 0 & 0 & 0 & 0 & 0 & -a_5 & 0 \\ 0 & 0 & 0 & 0 & 0 & 0 & 0 & 0 & -a_6 \end{pmatrix}, \tag{8}$$

and the eigenvalues associated to $J(E_0)$ are:
$\lambda_1 = -a_6$,
$\lambda_2 = -k_c$,
$\lambda_3 = -a_5$,

$\lambda_4 = -a_3,$
$\lambda_5 = -\mu_{ds},$
$\lambda_6 = -\mu_E,$
$\lambda_7 = -\frac{A}{3} + \frac{2^{\frac{2}{3}}Q}{6} + \frac{3^{-1}2^{\frac{1}{3}}(H-B)}{Q},$
$\lambda_8 = -\frac{A}{3} - (\frac{2^{\frac{2}{3}}Q}{12} + \frac{3^{-1}2^{\frac{1}{3}}(H-B)}{2Q}) - (\frac{2^{\frac{2}{3}}3^{\frac{1}{2}}Q}{12} - \frac{3^{-1}2^{\frac{1}{3}}(H-B)}{2Q})i,$
$\lambda_9 = -\frac{A}{3} - (\frac{2^{\frac{2}{3}}Q}{12} + \frac{3^{-1}2^{\frac{1}{3}}(H-B)}{2Q}) + (\frac{2^{\frac{2}{3}}3^{\frac{1}{2}}Q}{12} - \frac{3^{-1}2^{\frac{1}{3}}(H-B)}{2Q})i,$

where
$A = a_1 + a_2 + a_4,$
$B = a_1a_2 + a_1a_4 + a_2a_4,$
$C = 27a_1a_2a_4,$
$D = 27(a_4b_1k_2 + a_2k_{pin}k_{pout}),$
$E = b_1k_2 + k_{pin}k_{pout},$
$F = a_1^2 + a_2^2 + a_4^2,$
$G = 9A(B-E) - 2A^3 - C + D,$
$H = F + 3E,$
$Q = (G + (G^2 - 4(H-B)^3)^{\frac{1}{2}})^{\frac{1}{3}},$
and
$a_1 = k_1R_{ibo}^{Tot} + k_{pin} + \mu_p^c - k_0,$
$a_2 = k_2 + \mu_{T_c},$
$a_3 = k_{Ein} + \mu_E^{cyt},$
$a_4 = k_{pout} + \mu_p,$
$a_5 = k_{4m} + \mu_{Ip},$
$a_6 = k_{4p} + \mu_{Ids},$
$b_1 = k_1R_{ibo}^{Tot},$
$b_2 = k_5x_7 + \mu_{ds},$
$b_3 = k_5x_6 + k_3x_5 + \mu_E.$

Lemma 3.2. *If $Q > 0$ then,*
i. E_0 is locally asymptotically stable when $A > (2^{-\frac{1}{3}}Q + 2^{\frac{1}{3}}Q^{-1}(H-B))$.
ii. E_0 is a saddle point when $A < (2^{-\frac{1}{3}}Q + 2^{\frac{1}{3}}Q^{-1}(H-B))$.

Proof. Suppose $Q > 0$, then:
i. λ_8 and λ_9 will have negative real parts. Also, since a_3, a_5, a_6, k_c, μ_E, and μ_{ds} are real and positive, then the eigenvalues λ_i , $i = 1, 2, 3, ..., 6$ are negative real eigenvalues.
Lastly, λ_7 will be negative when $A > (2^{-\frac{1}{3}}Q + 2^{\frac{1}{3}}Q^{-1}(H-B))$. Thus, $\lambda_i, i = 1, 2, 3, 4, 5, 6, 7, 8, 9$ have negative real parts, hence E_0 is locally asymptotically stable.
ii. Claiming same for $\lambda_i, i = 1, 2, 3, 4, 5, 6, 8, 9$. Now if $A < (2^{-\frac{1}{3}}Q + 2^{\frac{1}{3}}Q^{-1}(H-B))$ then λ_7 will be positive. Hence E_0 is a saddle point. □

Observe that, decreasing the rate of influx (k_0) increases the value of A which leads to local stability of trivial equilibrium.

3.2.2. *Local stability of healthy equilibrium.* Using next generation method, we compute the basic replication number $\mathcal{R}_0$, which is the threshold parameter that measure the average number of new replicated copies generated by single virus when introduce in to a complete healthy cells over its entire period. In order to compute $\mathcal{R}_0$, we first write the system (2) in the form:

$$\begin{aligned} \frac{dX}{dt} &= \mathcal{F}(X) - \mathcal{V}(X), \\ \mathcal{V}(X) &= \mathcal{V}^-(X) - \mathcal{V}^+(X), \\ X &= (x_1, x_2, x_3, x_4, x_5, x_6, x_7, x_8, x_9)^T, \end{aligned} \tag{9}$$

where $\mathcal{F}, \mathcal{V}^+, \mathcal{V}^- : \mathbf{R}^9 \to \mathbf{R}^9$.
Considering the infected compartments x_1, x_2 and x_5, then by next generation method [20, 21], the associated matrices F for the new infection terms, and V for the remaining transmission terms at healthy equilibrium are, respectively, given by

$$F = \begin{pmatrix} 0 & 0 & 0 \\ k_1 R_{ibo} & 0 & 0 \\ 0 & 0 & 0 \end{pmatrix}, \quad V = \begin{pmatrix} k_{pin} + \mu_p^{cyt} + k_1 R_{ibo} - k_0 & -k_2 & -k_{pout} \\ 0 & k_2 + \mu_{Tc} & 0 \\ -k_{pin} & 0 & k_{pout} + \mu_p \end{pmatrix}.$$

Further,

$$FV^{-1} = \begin{bmatrix} 0 & 0 & 0 \\ q & u & w \\ 0 & 0 & 0 \end{bmatrix}$$

where,

$$\begin{aligned} q &= \frac{k_1 R_{ibo}(k_{pout} + \mu_p)}{[(k_{pin} + \mu_p^{cyt} + k_1 R_{ibo} - k_0)(k_{pout} + \mu_p) - k_{pin} k_{pout}]}, \\ u &= \frac{k_2 k_1 R_{ibo}(k_{pout} + \mu_p)}{(k_2 + \mu_{Tc})[(k_{pin} + \mu_p^{cyt} + k_1 R_{ibo} - k_0)(k_{pout} + \mu_p) - k_{pin} k_{pout}]}, \\ w &= \frac{k_{pout} k_1 R_{ibo}}{[(k_{pin} + \mu_p^{cyt} + k_1 R_{ibo} - k_0)(k_{pout} + \mu_p) - k_{pin} k_{pout}]}. \end{aligned}$$

The eigenvalues of the matrix FV^{-1} are $0, 0, u$. Thus, it follows that the basic replication number of the modified model is:

$$\mathcal{R}_0 = \rho(FV^{-1}) = \frac{k_2 k_1 R_{ibo}(k_{pout} + \mu_p)}{(k_2 + \mu_{Tc})[k_{pin}\mu_p + (\mu_p^{cyt} + k_1 R_{ibo})(k_{pout} + \mu_p) - (k_{pout} + \mu_p)k_0)]}, \tag{10}$$

where, ρ is called the spectral radius, $k_0 \geq 0$.

Lemma 3.3. *$\mathcal{R}_0$ exists iff $k_0 < \frac{k_{pout}\mu_p}{k_{pout}+\mu_p} + (\mu_p^c + k_1 R_{ibo})$.*

Observe that, increasing the rate of influx (k_0) also increases the value of $\mathcal{R}_0$. Likewise, decreasing k_0 decreases the value of $\mathcal{R}_0$. Applying Theorem 2 of [24], the following result is established.

Lemma 3.4. *The healthy equilibrium E_1 of the model (2) is locally asymptotically stable if $\mathcal{R}_0 < 1$, and unstable if $\mathcal{R}_0 > 1$.*

Biologically speaking, Lemma (3.4) implies that the replication can be controlled when $\mathcal{R}_0 < 1$, depending on the intial sizes of replication mechanisms in the model (2). It is noteworthy that increasing k_0 increases $\mathcal{R}_0$, and vice versa.

3.2.3. *Threshold Analysis.* In order to assess the impact of k_0, we differentiate $\mathcal{R}_0$ partially with respect to k_0, so we have:

$$\frac{\partial \mathcal{R}_0}{\partial k_0} = \frac{(k_{pout}+\mu_p)^2 k_2 k_1 R_{ibo}}{(k_2+\mu_{Tc})[k_{pout}\mu_p + (\mu_p^c + k_1 R_{ibo})(k_{pout}+\mu_p) - (k_{pout}+\mu_p)k_0]^2}. \quad (11)$$

Since all the model parameters are non-negative, then $\frac{\partial \mathcal{R}_0}{\partial k_0} > 0$, thus the following result.

Lemma 3.5. *The rate of influx of HCV into Huh-7 cell have detrimental impact in the system.*

3.3. **Global stability of healthy equilibrium.**

Lemma 3.6. *For system (2), the healthy equilibrium E_1 is globally asymptotically stable if $\mathcal{R}_0 < 1$ and $k_3 x_5 x_7 - k_{4p} x_9 \geq 0$.*

Proof. We use the comparison theorem to prove the global stability of the healthy equilibrium E_1. The rate of change of the variables x_1, x_2, and x_5 of system (2) can be written as:

$$\begin{pmatrix} \frac{dx_1}{dt} \\ \frac{dx_2}{dt} \\ \frac{dx_5}{dt} \end{pmatrix} = (F - V) \begin{pmatrix} x_1 \\ x_2 \\ x_5 \end{pmatrix} - \begin{pmatrix} 0 \\ 0 \\ k_3 x_5 x_7 - k_{4p} x_9 \end{pmatrix},$$

where F and V are as defined in Section 3.2. By positivity of solutions and system parameters for all $t \geq 0$, then

$$\begin{pmatrix} \frac{dx_1}{dt} \\ \frac{dx_2}{dt} \\ \frac{dx_5}{dt} \end{pmatrix} \leq (F - V) \begin{pmatrix} x_1 \\ x_2 \\ x_5 \end{pmatrix}$$

Whenever $k_3 x_5 x_7 - k_{4p} x_9 \geq 0$. By lemma 1 of [24] the eigenvalues of the matrix F - V all have negative real parts. Thus, the system (2) is stable whenever $\mathcal{R}_0 < 1$. Therefore,$(x_1, x_2, x_5) \to (0, \eta, 0)$ as $t \to \infty$. By the comparison theorem [24], it follows that $(x_1, x_2, x_5) \to (0, \eta, 0)$ and $(x_3, x_4, x_6, x_7, x_8, x_9) \to (0, 0, 0, 0, 0, 0)$ as

$t \to \infty$. Then $(x_1, x_2, x_3, x_4, x_5, x_6, x_7, x_8, x_9) \to E_1$ as $t \to \infty$. Hence, E_1 is globally asymptotically stable provided $\mathcal{R}_0 < 1$. □

3.3.1. *Existence of endemic equilibrium.* To provide the condition for the existence of infected (endemic) equilibrium (that is, when every mechanism is present) we define the force of infection to be

$$\lambda^* = k_1 R_{ibo} x_1^*. \tag{12}$$

Thus, solving system (2) at steady state gives:

$$\begin{aligned}
x_1^* &= \frac{\phi_2\lambda^* - \phi_1}{\phi_3} \\
x_2^* &= \frac{\lambda^*}{k_2 + \mu_{Tc}} \\
x_3^* &= \frac{k_2\lambda^*}{k_c(k_2 + \mu_{Tc})} \\
x_4^* &= \frac{k_2\lambda^*}{(k_2 + \mu_{Tc})(k_{Ein} + \mu_E^c)} \\
x_5^* &= (\mathcal{R}_0 - 1)\frac{\alpha\psi_1\lambda^*}{\xi(k_{4p} + \mu_{Ids})(\beta_1 - \beta_2)\rho} \\
x_6^* &= (\mathcal{R}_0 - 1)\frac{\alpha\psi_2\lambda^*}{\xi(k_{4m} + \mu_{Ip})(\beta_1 - \beta_2)\rho} \\
x_7^* &= 1 \\
x_8^* &= (\mathcal{R}_0 - 1)\frac{k_3\alpha\psi_1\lambda^*}{\xi(k_{4p} + \mu_{Ids})(k_{4m} + \mu_{Ip})(\beta_1 - \beta_2)\rho} \\
x_9^* &= (\mathcal{R}_0 - 1)\frac{k_5\alpha\psi_2\lambda^*}{\xi(k_{4m} + \mu_{Ip})(k_{4p} + \mu_{Ids})(\beta_1 - \beta_2)\rho},
\end{aligned} \tag{13}$$

where,

$$\begin{aligned}
\alpha &= k_{pin}\mu_p + (\mu_p^C + k_1 R_{ibo} - k_0)(k_{pout} + \mu_p) \\
\xi &= (k_2 + \mu_{Tc})\alpha - k_2 k_1 R_{ibo}(k_{pout} + \mu_p) \\
\rho &= k_{pin} + \mu_p^C - k_0 \\
\psi_1 &= k_{pin}\mu_{Tc}(\mu_{ds}(k_{4p} + \mu_{Ids}) + k_5\mu_{Ids}) \\
\psi_2 &= k_3 k_{4m} k_{pin}\mu_{Tc} \\
\beta_1 &= \frac{(\mu_{ds}(k_{4p} + \mu_{Ids}) + k_5\mu_{Ids})[k_{pin}(k_3 + \mu_p) - (k_0 - \mu_p^C)(k_3 + k_{pout} + \mu_p)]}{(k_{4p} + \mu_{Ids})\rho} \\
\beta_2 &= \frac{k_3 k_{4m} k_{4p} k_5}{(k_{4p} + \mu_{Ids})(k_{4m} + \mu_{Ip})} \\
\phi_1 &= \mu_{Tc}\xi(k_{4p} + \mu_{Ids})(\beta_1 - \beta_2)\rho \\
\phi_2 &= (\mathcal{R}_0 - 1)(k_2 + \mu_{Tc})k_{pout}\alpha\psi_1 \\
\phi_3 &= \xi\rho^2(k_{4p} + \mu_{Ids})(\beta_1 - \beta_2).
\end{aligned}$$

Substituting (13) into (12) leads to

$$a_{11}\lambda^* - a_{12} = 0, \tag{14}$$

where,

$$\begin{aligned} a_{11} &= k_1 R_{ibo}\phi_2 - \phi_3 \\ a_{12} &= k_1 R_{ibo}\phi_1 \end{aligned} \tag{15}$$

Hence, we have the following result.

Theorem 3.7. *Suppose $\mathcal{R}_0 > 1$, then the model (2) has a unique positive endemic equilibrium if a_{11} and a_{12} have the same sign.*

4. NUMERICAL SIMULATIONS

To illustrate the effect of plus-strand RNA in the model (2), we present the simulations of the model (2) using the parameter values in table 1 and at the time of transfection (i.e $t = 0$), we assume $x_i(0) = 0 \quad for \quad i = 2, 3, 4, 5, 6, 7, 8, 9$ and $x_1(0) = 500$ as used by Dahari et al [2]. The numerical result is shown in figure 2. We simulate the model (2) with different values of rate of influx (k_0) and observe a disparity in steady state level of total plus-strand RNA, synthesized plus-strand RNA in the cytoplasm, replicated plus-strand RNA in VMS, and NS5B (which is the key replication mechanism).

5. SENSITIVITY AND UNCERTAINTY ANALYSES

In this section, to quantify the impact of the variations of each parameter of the model, we use partial rank correlation coefficients (PRCC) to carry out a global sensitivity analysis [28, 29]. Furthermore, an uncertainty analysis is performed, using latin hypercube sampling (LHS). The analyses are carried out for the model using the parameter values and ranges in Table 1 and the associated reproduction number as the response function. Uniform distribution is assumed for the parameters of the model and also generate 1000 LHS samples.

A box plot of the $\mathcal{R}_0$ as a function of the LHS runs, as depicted in Figure 4, shows that the distribution of $\mathcal{R}_0$ lies within the interval $\mathcal{R}_0 \in [0.9999, 1.0008]$, with a mean of $\mathcal{R}_0 = 1.0003$. Moreover, Figure 5 shows that the rate of influx, k_0 of HCV plus-strand RNA (which is the viral particle) is the dominant PRCC-ranked parameter for the model and then followed by the rate of production of translation complex (T_c) and the rate of degradation, μ_p^{cyt}, of plus-strand RNA R_P^{cyt}. Thus, these simulations suggest that when k_0 increases, then the steady state level of total plus-strand RNA in the system, synthesization plus-strand RNA in the cytoplasm, replication copies of plus-strand RNA in VMS and NS5B also increase.

CONCLUSIONS

An extension of Dahari et al [2] model of sub-genomic HCV replication in Huh-7 cell is presented. The qualitative analysis shows that the model has three equilibria viz trivial equilibrium, healthy equilibrium and endemic equilibrium. The

trivial equilibrium could either be locally asymptotically stable or saddle point depending on certain threshold quantity. Basic replication number is obtained and found that the healthy equilibrium E_1 is globally asymptotically stable when $\mathcal{R}_0 < 1$ and unique positive endemic equilibrium exists when $\mathcal{R}_0 > 1$. Further, threshold analysis on $\mathcal{R}_0$ reveals that high rate of influx of plus-strand RNA can cause detrimental effect. It is shown that changing the rate of influx changes the steady state level of total plus-strand RNA in the system, synthesizes plus-strand RNA in the cytoplasm, replicates plus-strand RNA in VMS and NS5B (which is the key replication mechanism). It is observed, as depicted in Figure 3, that $\mathcal{R}_0$ is directly proportional to the rate of influx. Sensitivity and uncertainty analyses of the model (using the *basic replication number* ($\mathcal{R}_0$) as the response function) show that the top three PRCC-ranked parameters are the rate of influx (k_0) of HCV plus-strand RNA, the rate of production of translation complex (T_c) and the rate of degradation (μ_p^{cyt}) of plus-strand RNA R_P^{cyt}. Furthermore, the distribution of $\mathcal{R}_0$ is between [0.9999, 1.0008] with a mean of $\mathcal{R}_0 = 1.0003$.

REFERENCES

[1] Philippe R., Christophe H., Emmanuelle B., Denys B. and Malika A., Hepatitis C virus ultra-structure and morphogenesis, *Biology of the cell*, 96(2004), 103-108.

[2] Harel D., Ruy M. R., Charles M. R. and Alan S. P., Mathematical Modeling of Subgenomic Hepatitis C Virus Replication in Huh-7 Cells, *Journal of Virology*, 81(2007), 750-760.

[3] Nurgary S., Mathematical Modeling of Hepatitis C Virus Replication, *Heidelberg University*, 2012

[4] Spiegelman P., Extracellular evolution of replicating molecules, The neurosciences, *Rockefeller university*, New York, In F. O. Schmitt (ed.)(1970), 927.

[5] Wasley A. and Alter M. J., Epidemiology of Hepatitis C: geographic differences and temporal trends, *Semin liver Dis.*, 20(1),(2000) 1-16.

[6] Lohmann V., Korner F., Koch J., Herian U., Theilmann L. and Bartenschlager R., Replication of subgenomic hepatitis C Virus RNA in a hepatoma cell line,*Science*, 285(1999), 110-113.

[7] Bartenschlager R., Frase M. and Pietschmann T., Novel insights into hepatitis C virus replication and persistence, *Advances in virus research*, Academic press(2004), 71-180.

[8] Quinkert D., Bartenschlager R. and Lohmann V., Quantitative Analysis of the Hepatitis C Virus Replication Complex, *Journal of Virology*, 79(21)2005, 13594-13605.

[9] Ashfaq U. A., Javed T., Rehman S., Nawaz Z. and Riazuddin S., An overview of HCV molecular biology, replication and immune response, *Virology J.*, 8(161) 2011.

[10] Dubuisson J., Helle F. and Cocquerel L., Early steps of the hepatitis C virus life cycle, *Cellular Microbiology*, 10(4)2008, 821-827.

[11] Popescu C. and Dubuisson J., Role of lipid metabolism in hepatitis C virus assembly and entry, *Biol. Cell*, 102(2010) 63-74.

[12] Burlone M. E. and Budkowska, Hepatitis C virus entry: role of lopoprotein and cellular receptor, *J. of General Virology*, 90(2009), 1055-1070.

[13] Ma H., Leveque V., Witte D. A., Li W., Hendricks T., Clausen S. M., Cammack N. and Klumpp K., Inhibition of native hepatitis C virus replicase by nucleotide and non-nucleoside inhibitors, *Virology* 332(2005), 8-15.

[14] Chatterjee A., Guedj J. and Perelson A. S., Review Mathematical modelling of HCV infection: what can it teach us in the era of direct-acting antiviral agents?, *Antivaral Therapy*, 17(2012),1171-1182.

[15] Bartenschlager R. and Lohmann V., Replication of hepatitis C virus, *Journal of General Virology*, 81(2000), 1631-1648.

[16] Lavanchy D., Purcell R., Hollinger F. B., Howard C., Alberti A., Kew M., Dusheiko G., Alter M., Ayoola E., Beutels P., Bloomer R., Ferret B., Decker R., Esteban R., Fay O., Fields H., Fuller E. C., Grob P., Houghton M., Leung N., Locarnini S. A., Margolis H., Meheus A., Miyamura T., Mohamed M. K., Tandon B., Thomas D., Head H. T., Toukan A. U., Van D. P., Zanetti A., Arthur R., Couper M., D'Amelio R., Emmanuel J. C., Esteves K., Gavinio P., Griffiths E., Hallaj Z., Heuck C. C., Heymann D. L., Holck S. E., Kane M., Martinez L. J., Meslin F., Mochny I. S., Ndikuyeze A., Padilla A. M., Rodier G. M., Roure C., Savage F. and Vercauteren G., Global surveillance and control of hepatitis C, *Journal of Viral Hepatitis*, 6(1999), 35-47.

[17] Stuyver J. L., McBrayer R. T., Tharnish M. P., Hassan E. A., Chu K. C., Pankiewicz W. K., Watanabe A. K., Schinazi F. R. and Otto J. M., Dynamics of Subgenomic Hepatitis C Virus Replicon RNA Levels in Huh-7 Cells after Exposure to Nucleoside Antimetabolites, *Journal of Virology*, 77(19)2003, 10689-10694.

[18] Eigen M., Biebricher C. K., Gebinoga M. and Gardiner W. C., The hypercycle Coupling of RNA and protein biosynthesis in the infection cycle of an RNA bacteriophage, *Biochemistry*,30(46)1991, 11005-11018.

[19] Biebricher C. K., Eigen M. and Luce R., Kinetic analysis of template-instructed and de novo RNA synthesis by Qβ replicase, *J. Mol. Biol.*, 148(1981), 391-410.

[20] Nafiu H., Winter M., and A. B. Gumel, Qualitative Assessment of the Role of Public Health Education Program on HIV Transmission Dynamics, *Mathematical Medicine and Biology*, 28(2011), 245-270.

[21] Van den Driessche P. and Watmough J., Reproduction Numbers and Sub-Threshold Endemic Equilibria for Compartmental Models of Disease Transmission, *Math. Biosci.*, 180(2002), 29-48.

[22] Chu P. W. and Westaway E. G., Replication strategy of Kunjin virus:evidence for recycling role of replicative form RNA as template in semiconservative and asymmetric replication, *Virology*, 140(1985), 68-79.

[23] Dahari H., Feliu A., Garcia-Retortillo M., Forns X. and Neumann A. U., Second hepatitis C replication compartment indicated by viral dynamics during liver transplantation, *J. Hepatol*, 42(2005), 491-498.

[24] Lakshmikantham V. , Leela S. , and Martynyuk A. A., Stability Analysis of Nonlinear Systems, vol. 125, Marcel Dekker, New York, Ny, USA, 1989.

[25] Dahari H, Feinstone SM, Major ME, Meta-analysis of hepatitis C virus vaccine efficacy in chimpanzees indicates an importance for structural proteins. *Gastroenterology*, 139(2010), 965-974.

[26] Nikita V. I., Elena L. M., Ilya R. A., Pavel S. D., Vitaly A. L., Konstantin N. K., Dmitry I. T., Vitaly V. G., Maria G. S., Alexander M. S., Diana C., Lars K., Nikolay A. K., Vladimir A. I., A New Stochastic Model for Subgenomic Hepatitis C Virus Replication Considers Drug Resistant Mutants, *Plos One Journal*, 9(3)2014, 1-17.

[27] Hai-Feng H. and Na-Na S., Global Stability for a Binge Drinking Model with Two Stages, *Discrete Dynamics in Nature and Society*,2012, 1-15.

[28] Blower, S.M. Dowlatabadi, H., Sensitivity and uncertainty analysis of complex models of disease transmission: an HIV model, as an example, *International Statistical Review* 2 (1994) 229–243.

[29] Hussaini, N., Lubuma, J. M-S., Barley K. and Gumel, A.B.: Mathematical analysis of a model for AVL–HIV co-endemicity. *Mathematical Biosciences*. 271 (2016): 80-95.

[30] WHO, World Health Organisation, Hepatitis C FactSheet, accessed 10th March, 2019. www.who.intnews-roomfact-sheetsdetailhepatitis-c.

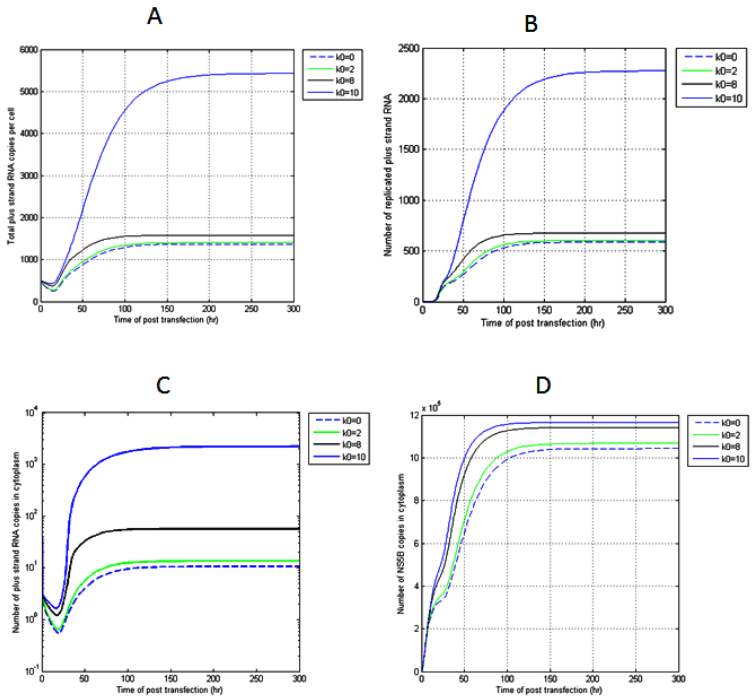

FIGURE 2. Simulations of the model (2) showing the disparity in steady state level of (A) Total plus-strand RNA in the system, (B) Synthesized plus-strand RNA in the cytoplasm, (C)Replicated plus-strand RNA in VMS, and (D) NS5B (which is the key replication mechanism).

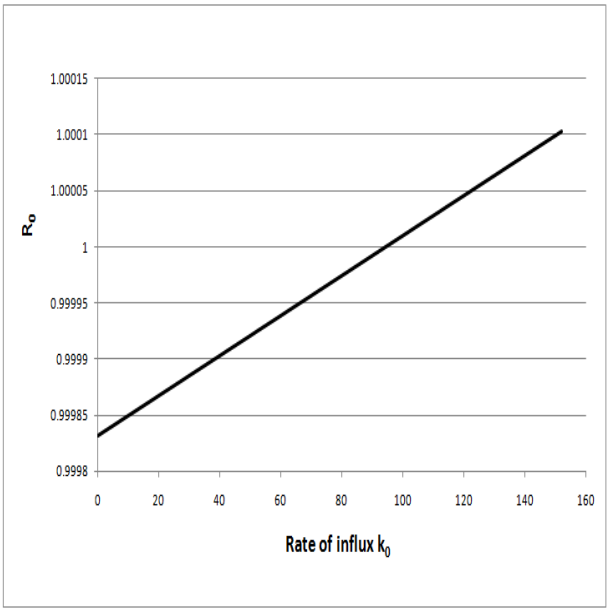

FIGURE 3. Graph showing increase in $\mathcal{R}_0$ due to increase in rate of influx

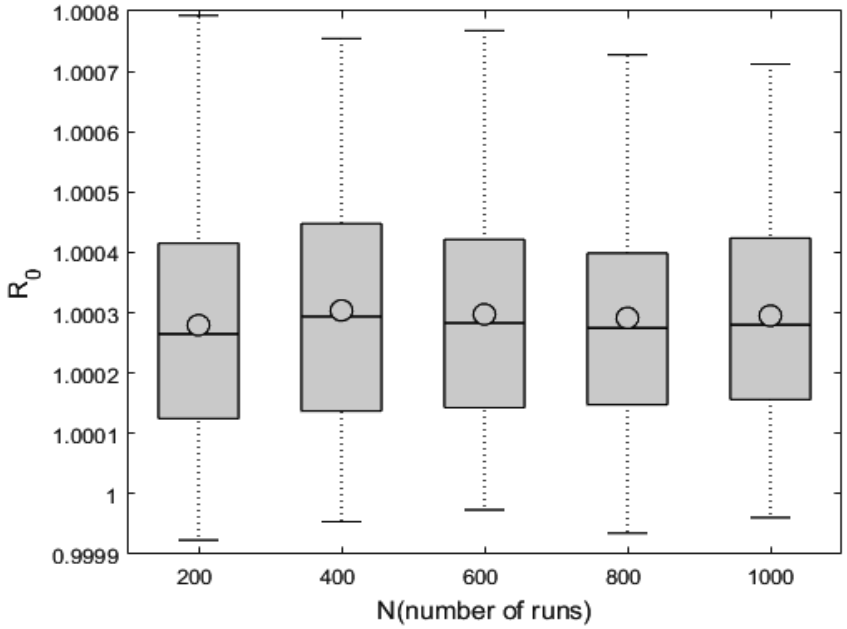

FIGURE 4. Box plot of $\mathcal{R}_0$ as a function of the LHS runs. Parameter values used are as in Table 1.

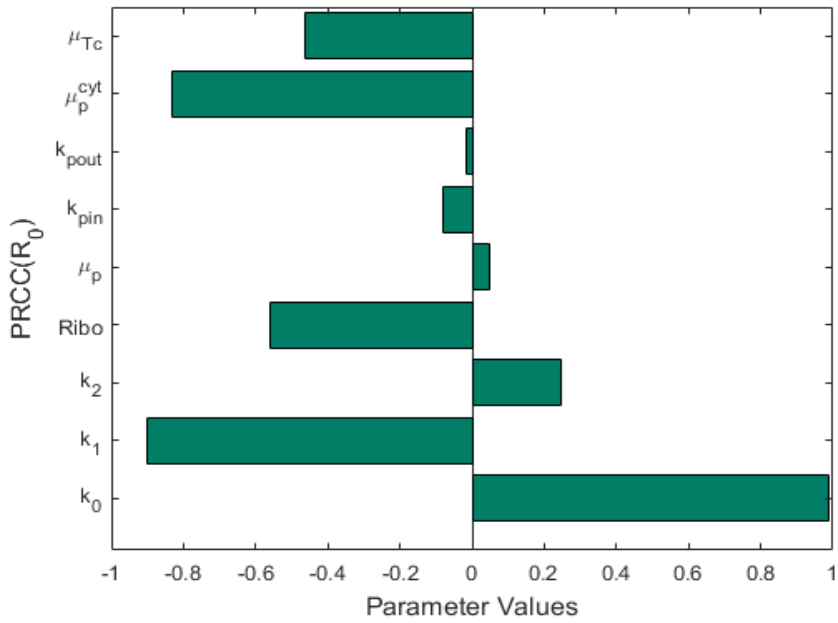

FIGURE 5. Distribution of PRCC values for the model (2) using $\mathcal{R}_0$ as the response function. Parameters and ranges used are as in Table 1.